21st Australasian Fluid Mechanics Conference
Adelaide, Australia
10-13 December 2018

A numerical study for passive turbulent drag reduction via shallow dimples

J. H. Ng[1], R. K. Jaiman[2] and T. T. Lim[1]

[1]Department of Mechanical Engineering
National University of Singapore, 117575, Singapore

[2]Department of Mechanical Engineering
University of British Columbia, Vancouver, BC V6T 1Z4, Canada

Abstract

The present numerical work, which adopts a wall-resolved large-eddy simulation (LES) approach, focuses on two aspects: (i) Setting up an efficient and reliable numerical framework to simulate turbulent flows over a dimpled surface for a wide range of Reynolds number, and (ii) Determining the correlation between the drag property and the mean flow pattern. The present simulations in a channel domain are able to reproduce the qualitative trend of percentage drag reduction as a function of the flow Reynolds number that is observed in the in-house experiment. The current LES shows up to $\approx 2\%$ drag reduction at the highest Reynolds number considered. The results confirm that the drag property of a dimpled surface correlates strongly with the nature of flow separation near the dimple. At higher Reynolds number, the flow recirculation region shrinks due to upstream shifting of the flow reattachment location, leading to a lower form drag contribution. On the other hand, regulating the form drag component by shear-deforming the dimple along the flow direction is associated with the shifting of the stagnation point, instead of the flow reattachment location.

Introduction

The idea of surface contouring for turbulent drag reduction has been explored over the years [7]. Unfortunately, the practicality of the available techniques has been a major concern because of reliability and maintainability issues. In this regard, there are still ongoing efforts to explore alternative surface textures that could provide persistent turbulent drag reduction over the course of operation. Recently, there is a keen interest on studying the drag property of a dimpled surface [8, 18], which is well-known for enhancing convective heat transfer with a relatively small penalty on the pressure drop [2, 3, 9]. However, consensus regarding the drag reduction performance is still lacking, mainly because the flow over a dimpled surface is influenced by several geometric and flow parameters.

A dimpled surface is generally formed by an array of spherical indentations (a.k.a circular dimples) of certain depths. Heat transfer applications often favor deep dimples with depth–to–diameter ratios of 0.2 to 0.5. On the other hand, the use of shallow dimples with depth–to–diameter ratios of 0.1 or less has shown promising prospects for reducing turbulent drag in a few experimental works [14, 17]. These studies found that the drag reduction generally enhances with the Reynolds number, and up to 5% reduction has been reported. In addition, a recent experiment showed that skewing the dimple wall along the flow direction can mitigate the form drag associated with flow separation in the dimple, leading to a better drag reduction performance [16]. To the best of knowledge, numerical investigations [3, 8, 12, 15, 19] thus far have yet to report any drag reduction produced by a dimpled surface.

The primary challenge of numerical simulations of turbulent flows is to resolve the important scales of motions faithfully, which inevitably entails a higher computational cost. Since drag reduction is typically observed at sufficiently high Reynolds number, earlier direct numerical simulations (DNS) [8, 19] that were performed at low to moderate Reynolds numbers would not be able to demonstrate the drag reduction potential of a dimpled surface. While some of the numerical works have resorted to approaches such as Reynolds-averaged Navier–Stokes (RANS) [12] or Detached-eddy simulation (DES) [3, 15] to simulate at a higher range of Reynolds number, the fidelity of these approaches is strongly influenced by the turbulence modeling implementation. As pointed out in a recent comparison [1], the various conventional RANS turbulence models can lead to different flow patterns on a dimpled surface. Furthermore, there is a concern on the adequacy of conventional turbulence models in resolving the near-wall flow field near a textured surface. Failure to overcome these limitations will undoubtedly impede the elucidation of the underlying mechanism.

An earlier numerical work [15] demonstrated that the DES approach can predict large scale flow features reasonably well, and produce a correct qualitative trend of form drag versus Reynolds number as observed in the experiment. However, the same work revealed that a RANS modeled wall region tends to yield erroneous computation of viscous drag that does not corroborate with the experimental trend. These findings motivated the current numerical study based on the wall-resolved large-eddy simulation (LES) approach. The rationale of adopting the LES approach is to achieve a balance between accuracy and efficiency, so that the simulations can reproduce the qualitative trends over a range of Reynolds number as determined from the in-house experiment [14]. The improved numerical framework can then provide a more comprehensive set of data to scrutinize the effects of dimples, and to study other potential dimple geometries.

Problem description

The dimple array is studied in a fully-developed turbulent channel flow setting driven by a constant flow rate (CFR). Accordingly, the main parameter that characterizes the flow is the bulk Reynolds number $Re_m = U_m\delta/\nu$, where U_m is the bulk streamwise velocity, δ is the channel half-height, and ν is the fluid kinematic viscosity. An alternative Reynolds number $Re_H = U_c H/\nu$, where U_c is the centerline velocity and $H = 2\delta$ is the channel height, is also defined for ease of benchmarking with the experiment [14]. In the non-dimensional form, the governing equations in the present context can be expressed as follows:

$$\nabla \cdot V = 0 \tag{1}$$

$$\frac{\partial V}{\partial \mathcal{T}} + V \cdot \nabla V = -\nabla p + \frac{1}{Re_m}\nabla^2 V + \mathscr{F} e_x \tag{2}$$

where $V = (u, v, w)$, p and $\mathcal{T}$ are the non-dimensional velocity vector, pressure and time, respectively. u, v, and w are the respective components of V in the streamwise (x), wall-normal (y), and spanwise (z) directions. $\mathscr{F} > 0$ is a prescribed external force to drive the flow through the channel, and e_x is the unit

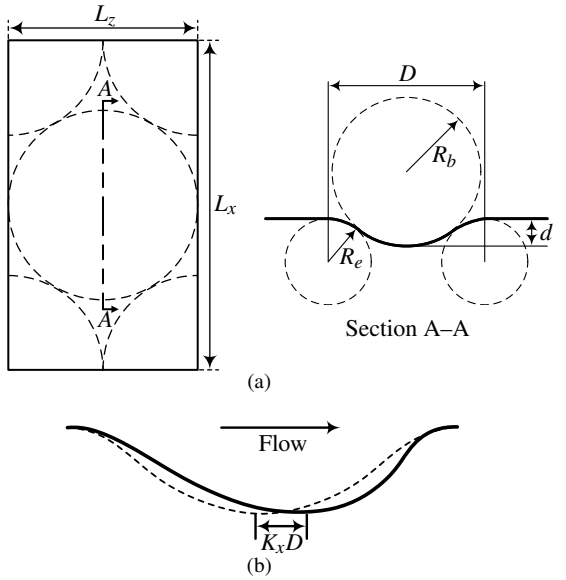

Figure 1: (a) Plan view of the dimpled wall, and section view of the circular dimple geometry. (b) Asymmetric dimple skewed in the flow direction as indicated by a parameter K_x.

vector in the x direction. In the current CFR setting, $\mathscr{F}$ is adjusted dynamically to achieve the desire flow rate through the channel. The change in mean drag caused by the dimple array is deduced from the difference of $\overline{\mathscr{F}}$ with respect to the value belonging to the baseline configuration at the same Re_m and flow rate. Aside from being consistent with the experiment [13], this method yields a lower uncertainty as compared to evaluating the change in mean drag directly from the walls. In most cases, the uncertainty is well within $\pm 1\%$ when estimated with a 95% confidence level. To model a fully-developed channel flow, periodic boundary condition is applied in the x and z directions, and a no-slip condition is enforced on the two walls. The streamwise and spanwise extents of the computational domain, denoted as L_x and L_z respectively, are determined from the geometry of the dimple array discussed in the next section.

Dimple geometry

Similar to the experiment, the bottom wall comprises of the dimple array while the opposite wall remains smooth. With reference to Section A–A depicted in figure 1(a), each circular dimple is characterized by four geometric parameters: Diameter D, depth d, edge radius R_e, and base radius R_b. In this numerical work, $D = 5\delta$, $d = 0.05D$, $R_e = 4.21\delta$, and $R_b = 8.415\delta$. A staggered array of circular dimples at the maximum coverage ratio of 90.7% is considered, where coverage ratio is defined as the percentage of the total planar area occupied by the dimple array. Due to the use of periodic boundary condition in the wall-parallel directions, L_x and L_z are adjusted to accommodate an appropriate periodic representation the dimple array. Figure 1(a) shows a plan view of the truncated dimple array with associated domain extents of $L_x = \sqrt{3}D$ and $L_z = D$. The corresponding baseline configurations with two plane walls are also simulated with the same domain size for a fairer assessment of the drag reduction performance. Asymmetric dimple as depicted in figure 1(b) is generated by shear-deforming the circular dimple along the flow direction according to a function described in [3]. The asymmetric dimple is characterized by a factor K_x, where a positive value indicates a downstream skewing and vice versa. The present work considers five cases with $-0.2 \leq K_x \leq 0.2$ at an increment of 0.1, inclusive of the symmetric case denoted as $K_x = 0$.

Numerical setup

The present LES simulations are performed using the open source flow solver *nek5000* [6]. The governing equations are discretized in space by a 7^{th} order spectral element method. Since this method combines the accuracy of the spectral method, and the generality of the finite element method, it is well-suited for simulating turbulent channel flows over dimples that are both geometrically and physically complex. Here, a $\mathbb{P}_N - \mathbb{P}_N$ formulation is used where both the velocity and pressure field are constructed in the same polynomial space. Time integration is performed via a third-order operator-integration-factor splitting (OIFS) method. Specific formulation and implementation details can be found in [5] and references therein. The LES implementation is based on a revised version of the dynamic Smagorinsky model described in [10]. In all simulations, the test-to-grid filter width ratio is set at ≈ 1.08.

To cross-check with the experiment [14], simulations of the symmetric dimples are conducted at various Reynolds numbers Re_m ranging from 2800 to 35000, or $6500 < Re_H < 79000$. In terms of the friction Reynolds number $Re_\tau = u_\tau \delta/\nu$, where u_τ is the friction velocity, the range is from ≈ 180 to ≈ 1645. Note that Re_H and Re_τ are derived with respect to the baseline configuration with two plane walls. The asymmetric dimples are only simulated at $Re_m = 2800$ where extensive flow reversal has been observed [15]. Since the accuracy of LES is contingent on the mesh design, the mesh for the simulation at each Re_m is first tuned based on the plane channel configuration. These preliminary simulations also yield the necessary data for computing the amount of drag reduction, and provide the initial condition for the corresponding dimpled channel simulation.

The plane channel domain consists of a structured hexahedral mesh with uniform element size distribution in the x and z directions. The element size along the y direction is prescribed by a hyperbolic tangent function to cluster more grid points near the two walls. In all the baseline configurations, the first grid point adjacent to the wall is at $y^+ = 0.3 \sim 0.5$, while the grid resolution Δy^+ near the centerline is around $30 \sim 50$. For the corresponding dimpled channel, the same hexahedral mesh is stretched in the y direction to conform to the geometry of the dimple array. Table 1 summarizes the simulation parameters of the configurations at various Re_m. It is observed that at sufficiently high Reynolds number beyond $Re_m = 20000$ or $Re_\tau \approx 1000$, the grid sensitivity diminishes. Hence, only the grid resolution in the y direction is increased when $Re_m > 20000$ to mitigate the increasingly higher computational cost.

Re_m	Re_H	N_x	N_y	N_z	Δt^*	T^*_{avg}
2800	6500	141	71	85	0.005	1800
6900	15800	211	85	127	0.0025	800
11000	25000	295	113	197	0.0025	700
15000	34100	393	169	267	0.001	500
20000	45500	561	197	337	0.001	300
25000	56600	561	211	337	0.001	300
30000	67700	561	225	337	0.001	300
35000	79000	561	239	337	0.001	300

Table 1: Summary of simulation parameters used in the present LES study. Here N_i is the number of grid points in the i direction, Δt^* and T^*_{avg} are the normalized time step size and time-averaging period, respectively.

Results and discussions

LES validation

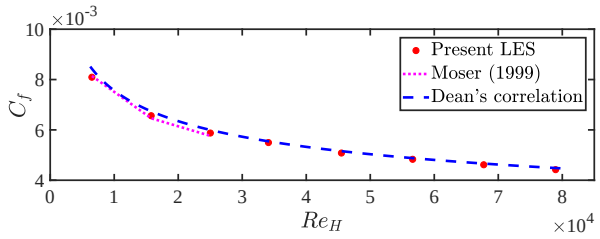

Figure 2: Comparison of skin friction coefficients computed from the present LES of the baseline turbulent channel flows at various Re_H with the empirical Dean's correlation.

For the purpose of validation, the skin friction coefficients C_f computed from the present LES of the baseline configurations are benchmarked against the values evaluated from the empirical Dean's correlation [4]. As illustrated in figure 2, the C_f values of the present LES match fairly well with Dean's suggested correlation. Those at the three lowest values of Re_H also have a close agreement with the available DNS data [11]. Although the dimples are relatively shallow, it is worth noting that their presence might affect the LES accuracy to some extent, especially at the lower range of Re_m. In the case of symmetric dimples at $Re_m = 2800$, it is found that LES under-predicts the percentage change in drag by about 1% as compared to DNS.

Drag reduction performance

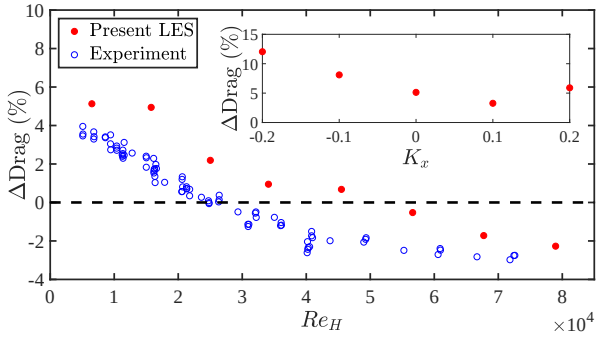

Figure 3: Percentage change in drag as a function of Re_H. (Inset) Percentage change in drag against K_x at $Re_m = 2800$.

Figure 3 compares the percentage change in drag ($\%DR$) at various Re_H between the present LES and the experimental data [14]. It can be observed that the two sets of data exhibit the same qualitative trend: $\%DR$ reduces at higher Re_H. However, it is noted that the simulated $\%DR$ is about 0.5% to 2% higher. As for the asymmetric dimples simulated at $Re_m = 2800$, the optimum K_x (with the least increase in drag) falls in the vicinity of 0.1 (see the inset in figure 3). Although not shown here, the improved drag performance at $K_x = 0.1$ corresponds to the lowest form drag, while the worst drag performance occurs when $K_x = -0.2$ at which the form drag is the highest. Interestingly, the viscous drag shows relatively small dependence on K_x as the variation is within 3% among the different configurations. This implies that changing the wall slope has no significant impact on the total viscous drag. Thus, it is likely that shear-deforming the dimple would not be effective in situations where the relative contribution of form drag is already small.

Flow pattern

Figure 4 depicts the flow patterns in the form of mean skin friction lines associated with dimples undergoing different degree of shear deformation along the flow direction. It can be observed that skewing the dimples mainly causes a shifting of the stagnation point, while the flow reattachment location is marginally affected. As K_x increases, the stagnation point shifts downstream until it coalesces with the reattachment location. At $K_x = 0.2$, the mean flow assumes a simple converging-diverging pattern as illustrated in figure 4(e). Despite the absence of flow separation, the total drag is still higher when compared to the case with $K_x = 0.1$. The reason is that the form drag is higher due to flow impingement on the downstream half of the dimple that has a steeper wall slope. On the other hand, figure 5 shows that increasing Re_m with $K_x = 0$ (symmetric dimples) causes the flow reattachment location to shift upstream, until it merges with the stagnation point beyond $Re_m = 20000$. The diminishing of flow recirculation at higher Re_m leads to a more symmetrical pressure distribution between the upstream and downstream sections of the dimple indentation. In turn, the relative contribution of form drag becomes smaller at higher Re_H.

Conclusions

LES study of fully-developed turbulent channel flows over a dimpled surface has been successful in reproducing the qualitative trend of percentage change in drag against Re_H measured in the experiment. By examining the mean flow pattern, it is found that increasing Re_H causes the flow reattachment location to shift upstream which helps to reduce the extent of flow recirculation and the form drag. On the other hand, shear-deforming the dimple along the flow direction at $Re_m = 2800$ mainly alters the form drag by shifting the stagnation location, with little effect on the viscous drag.

Acknowledgements

The current research work is supported by a grant from the Ministry of Education, Singapore. The computational work for this article was fully performed on resources of the National Supercomputing Centre, Singapore (https://www.nscc.sg).

References

[1] Amsha, K. A., Craft, T. J. and Iacovides, H., Computational modelling of the flow and heat transfer in dimpled channels, *Aeronautical Journal*, **121**, 2017, 1066–1086.

[2] Burgess, N. K. and Ligrani, P. M., Effects of dimple depth on channel Nusselt numbers and friction factors, *Journal of Heat Transfer*, **127**, 2005, 839–847.

[3] Chen, Y., Chew, Y. T. and Khoo, B. C., Enhancement of heat transfer in turbulent channel flow over dimpled surface, *International Journal of Heat and Mass Transfer*, **55**, 2012, 8100–8121.

[4] Dean, R. B., Reynolds number dependence of skin friction and other bulk flow variables in two-dimensional rectangular duct flow, *Journal of Fluids Engineering*, **100**, 1978, 215–223.

[5] Fischer, P. F., Kruse, G. W. and Loth, F., Spectral element methods for transitional flows in complex geometries, *Journal of Scientific Computing*, **17**, 2002, 81–98.

[6] Fischer, P. F., Lottes, J. W. and Kerkemeier, S. G., Nek5000, `http://nek5000.mcs.anl.gov`, 2008.

[7] Gad-el-Hak, M., Drag reduction, in *Flow Control: Passive, Active, and Reactive Flow Management*, Cambridge University Press, New York, 2000, 205–228.

[8] Lienhart, H., Breuer, M. and Köksoy, C., Drag reduction by dimples? - A complementary experimental/numerical

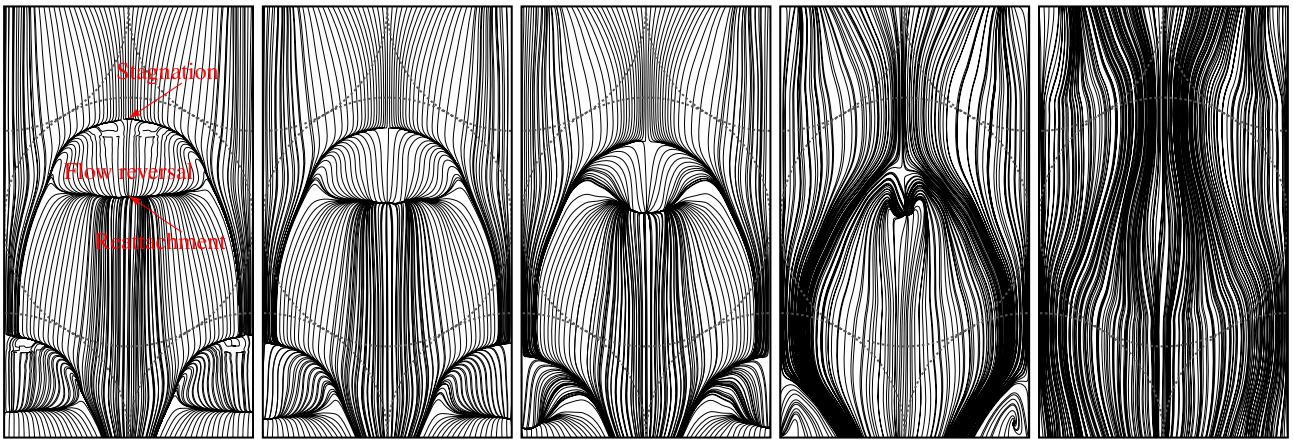

Figure 4: Mean skin friction lines on the dimple wall under different degree of shear-deformation along the flow direction at $Re_m = 2800$: (a) $K_x = -0.2D$, (b) $K_x = -0.1D$, (c) $K_x = 0.0D$, (d) $K_x = 0.1D$, and (e) $K_x = 0.2D$. Flow is from top to bottom.

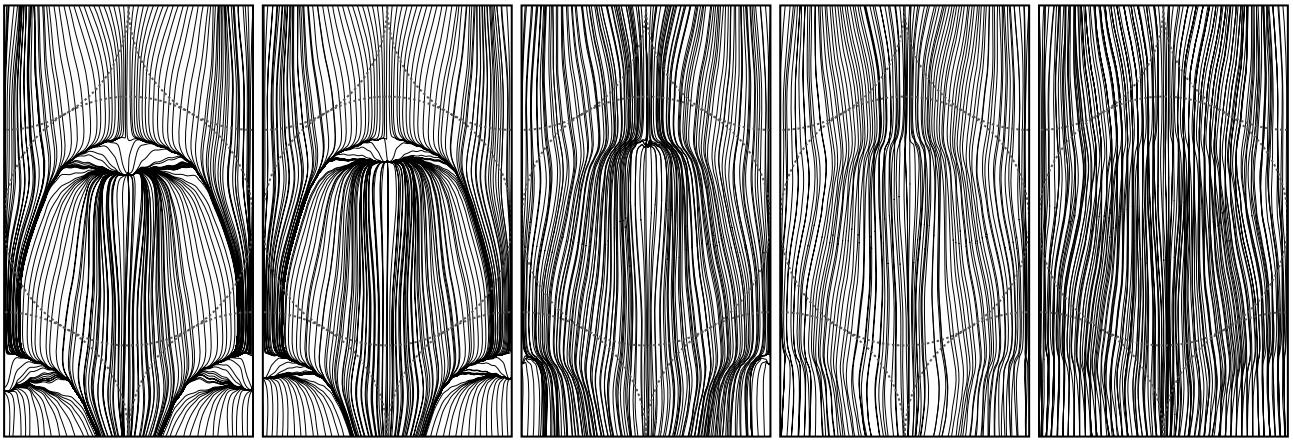

Figure 5: Mean skin friction lines on the dimple wall without shear-deformation ($K_x = 0$) along the flow direction at selected Re_m: (a) $Re_m = 6900$, (b) $Re_m = 11000$, (c) $Re_m = 20000$, (d) $Re_m = 25000$, and (e) $Re_m = 35000$. Flow is from top to bottom.

investigation, *International Journal of Heat and Fluid Flow*, **29**, 2008, 783–791.

[9] Ligrani, P. M., Burgess, N. K. and Won, S. Y., Nusselt numbers and flow structure on and above a shallow dimpled surface within a channel including effects of inlet turbulence intensity level, *Journal of Turbomachinery*, **127**, 2005, 321–330.

[10] Lilly, D. K., A proposed modification of the Germano subgrid-scale closure method, *Physics of Fluids A*, **4**, 1992, 633–635.

[11] Moser, R. D., Kim, J. and Mansour, N. N., Direct numerical simulation of turbulent channel flow up to $Re_\tau = 590$, *Physics of Fluids*, **11**, 1999, 943–945.

[12] Rao, Y., Feng, Y., Li, B. and Weigand, B., Experimental and numerical study of heat transfer and flow friction in channels with dimples of different shapes, *Journal of Heat Transfer*, **137**.

[13] Tay, C. M., Determining the effect of dimples on drag in a turbulent channel flow, in *49th AIAA Aerospace Sciences Meeting*, American Institute of Aeronautics and Astronautics, Orlando, Florida, 2011.

[14] Tay, C. M. J., Khoo, B. C. and Chew, Y. T., Mechanics of drag reduction by shallow dimples in channel flow, *Physics of Fluids*, **27**, 2015, 035109–22.

[15] Tay, C. M. J., Khoo, B. C. and Chew, Y. T., Use of DES in mildly separated internal flow: Dimples in a turbulent channel, *Journal of Turbulence*, **18**, 2017, 1180–1203.

[16] Tay, J. and Lim, T. T., Drag reduction with non-axisymmetric dimples, in *35th AIAA Applied Aerodynamics Conference*, American Institute of Aeronautics and Astronautics, Denver, Colorado, 2017.

[17] van Nesselrooij, M., Veldhuis, L. L. M., van Oudheusden, B. W. and Schrijer, F. F. J., Drag reduction by means of dimpled surfaces in turbulent boundary layers, *Experiments in Fluids*, **57**.

[18] Veldhuis, L. and Vervoort, E., Drag effect of a dented surface in a turbulent flow, in *27th AIAA Applied Aerodynamics Conference*, American Institute of Aeronautics and Astronautics, San Antonio, Texas, 2009.

[19] Wang, Z., Yeo, K. S. and Khoo, B. C., DNS of low Reynolds number turbulent flows in dimpled channels, *Journal of Turbulence*, **7**, 2006, 1–31.